Asian Journal of Chemistry; Vol. 34, No. 10 (2022), 2597-2603

ASIAN JOURNAL OF CHEMISTRY

https://doi.org/10.14233/ajchem.2022.23836

Comparative Adsorbent Studies using Pyrolyzed Materials Prepared from Custard Apple (*Annona squamosa*) Leaves in Removal of Fluoride from Wastewater

CHINTHAYYANAIDU RUDRAM[1,*], L. PARTHA PRAVEEN[1] and P. DINESH SANKAR REDDY[2]

[1]Department of Chemical Engineering, JNTUA College of Engineering, Ananthapuramu-515002, India
[2]Department of Chemical Engineering, NIT Andhra Pradesh, Tadepalligudem-534101, India

*Corresponding author: E-mail: chintu4407@gmail.com

Received: 16 March 2022; *Accepted*: 17 June 2022; *Published online*: 19 September 2022; AJC-20962

Pyrolyzed materials (biochar) obtained from the leaves of custard apple (*Annona squamosa*) at 800 ºC in open air (OPA) and in presence of inert gas (IGPA) were used as adsorbent materials. The effect of different parameters such as particle size, agitation speed, pH, contact time, adsorbent dosage, initial fluoride concentration and temperature on fluorine adsorption on *Annona squamosa* as the adsorbent has been investigated. At pH 7, the optimized factors were contact period (30 min), the agitation speed (500 rpm) and the adsorbent dosage (1.5 g per 50 mL of fluoride water). A maximum fluoride removal efficiency of 93% in the case of OPA and 96% in the case of IGPA was achieved. Adsorption isotherm modeling studies show that the adsorption onto OPA followed Dubinin-Raudskevitch isotherm model,whereas IGPA followed Langmuir isotherm model, respectively. Thermodynamic parameters such as ΔH^o, ΔG^o and ΔS^o were also estimated to ascertain the reaction is endothermic. In case of kinetics, pseudo-second order is the best fit for both OPA and IGPA. The SEM, FTIR and XRD patterns of the adsorbents were also recorded to have a greater comprehension of the adsorption process mechanism.

Keywords: Fluoride removal, Adsorption process, Custard apple leaf, Isotherms.

INTRODUCTION

Groundwater fluoride ion contamination is considered to be the most serious problem globally [1]. Fluorine is the most electronegative element and never be obtained in its elemental form and always present in the form of fluoride minerals. Due to its strongest electronegativity in nature, fluoride gets attracted towards calcium in bones and teeth due to its universally endorsed electropositive nature. Health issues caused by excess fluoride in aqueous solution are dental and skeletal fluorosis and deformation of bones [2]. India is one of the 23 countries where health problems are caused due to groundwater contaminated with fluoride ions. A ground breaking report from UNICEF has recognized the problem due to fluoride contamination in 177 districts from 20 provinces in India [3]. Fluoride presence has been detected in number of rivers in India and their identifiable concentration levels varied between 0.1 and 12 ppm. As a matter of fact, the drinking water fluoride concentration is limited to 1.0 to 1.5 mg/L [4].

To reduce the fluoride level in aqueous solutions, various defluoridation techniques exist, including coagulation and precipitation, ion exchange, membrane separation and adsorption method. Each approach has some advantages and limitations and worked productively under ideal conditions for the removal of fluoride [5].

Many inexpensive adsorbents were employed for the removal of fluoride ions for examples clays, soils, alumina, bone char, calcite, brick powder red mud, modified chitosan, activated carbon, activated kaolinites, oxides ores, *etc.* [6]. The majority of the substances used as adsorbents have extremely low acceptable limits in drinking water, above which they are harmful to people. With the exception of calcium and magnesium, which have a considerably larger permitted range in the drinking water, there is always a chance that these chemicals leach into the water and cause health problems. Other adsorbents that do not harm human body mechanisms in any way are being investigated. But, in some cases cost of the adsorbents, specificity of pH range and generation of secondary sludge are the major drawbacks. It is necessary to work in this area to change fluoride with a different chemical that doesn't contain aluminium in order to increase the affinity of calcium for it. Although

natural adsorbents, clay and soil-based adsorbents are non-toxic after usage in any way, however, it is still difficult to remove fluoride due to their poor capacity [7,8].

The objective of this work is to explore the attainability of an optional, minimal effort and novel bioadsorbents for the defluoridation in an aqueous solution effectively. Since the plant materials are the suitable precursors for the production of biochars possessing high surface areas and pore volumes, a range of pore size distribution, appropriate hardness and bulk density. Morever, the preparation of biochar by different techniques also plays an important role in the adsor-ption capacity [9,10]. Thus, the pyrolyzed materials (biochar) generated from the leaves of custard apple (*Annona squamosa*) in open air at 800 ºC (OPA) and in presence of inert gas (IGPA) were employed as a bioadsorbents to reduce the fluoride level employing batch process from an aqueous solution.

EXPERIMENTAL

All the chemicals and reagents used were of commercially available analytical grade (Fisher Scientific). Leaves of custard apple (*Annona squamosa*) were collected from the campus of the JNTUA College of Engineering, Ananthapuramu, India. Leaves were washed thoroughly to remove the foreign dirt and sun dried for few days to remove the moisture content. The dried leaves were crushed into small pieces and finely powdered using mortar and pestle. The washed powdered leaf material was the pyrolyzed in muffle furnace (Thermo-Fisher Scientific, USA) at 800 ºC for 8 h. This powder was screened with 50 to 400 No. BIS Sieves. This powder is used for fluorine removal named as open air pyrolyzed adsorbent (OPA).

Inert gas pyrolyzed leaf powder: The washed powdered dried leaves was thermal pyrolyzed in the presence of N_2 in a inert gas furnance at 800 ºC for 8 h. The biochar powder was screened with 50 to 400 No. BIS sieves. This powder was used for fluorine removal and named as inert gas pyrolyzed adsorbent (IGPA).

Preparation of stock solution: The fluoride stock solution, 2.21 g of NaF was mixed with 1 L deionised water. The aliquotes concentrations of 2 to 10 ppm were made from the stock solution.

Characterization: Fluoride high range, HI 98739 was used to determine the fluoride concentration (Henna Instruments). A digital pH metere (Elico-LI 617) was used to measure the pH. The FT-IR spectrophotometer (Perkin-Elmer Frontier MIR) was used to record the FTIR patterns within the ranges of 4000-400 cm^{-1} and the XRD-Panalytical (X'Pert3 Powder) used to record the XRD patterns of the adsorbent before and after the adsorption. The surface morphology of the adsorbent before and after the treatment of fluoride solution were carried out using Zeiss make ULTRA 55 model field emission scanning electron microscope (FESEM).

Batch adsorption: Fluoride removal was examined using adsorbents with various parameters such as pH, contact time, particle size, temperature, adsorbent dosage and initial concentration. All of the experiments were carried out using batch mode adsorption. These experiments were conducted in conical flasks (250 mL) at different agitation speeds with the help of magnetic stirrer. The solution was filtered using Whatman filter paper after agitation with a magnetic stirrer and the filtrate was used for fluoride analysis. All experiments have been carried out twice. The fluoride concentration solution was determined before and after adsorption using the fluoride meter. At the optimum values the removal of fluoride was high compared to other values during the variation of parameters. During the experimentation, the optimum values for initial concentration, particle size, contact time, temperature, pH and adsorbent dosage were estimated.

RESULTS AND DISCUSSION

Effect of adsorbent dosage and initial concentration: The effect of adsorbent dosages for the removal of fluoride ions were studied by varying adsorbent dosages from 0.25 g to 2.0 g of both adsorbents (OPA and IGPA) when initial fluoride concentration was 10 mg/L, pH of the solution was 7, temperature was maintained constant at 303 K, contact time of 30 min and size of adsorbent was 41.5 µm. The effects of adsorbent dosage of both adsorbents on the percentage of removal of fluoride are shown in Fig. 1, which indicated that the percentage removal of fluoride increases with increasing adsorbent dosage. The removal percentage of fluoride increased from 14% to 93% in case of OPA, while in case of IGPA, the removal increased from 19% to 96%, when the adsorbent dosage was increased from 0.25 g to 1.5 g per 50 mL of solution. An increase in percentage removal of fluoride can be attributed to the increase in available number of active adsorption sites on the adsorbent surface because of increasing adsorbent dosage. Even after increasing the adsorbent dosage from 1.5 g to 2.0 g there was no much increase in removal of fluoride percentage. This is due to a decrease in the availability of active sites, which causes adsorbent particle overlapping, limiting the active surface area available.

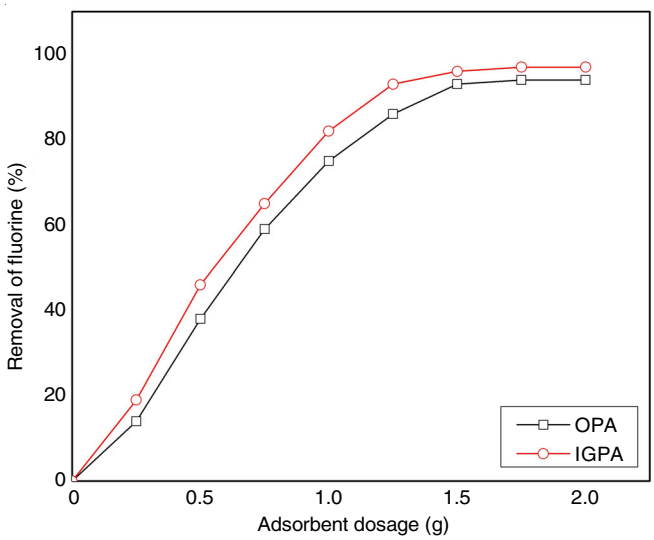

Fig. 1. Effect of adsorbent (OPA and IGPA) dosage on % removal of fluorine ions

Effect of particle size: The influence of average particle size of the adsorbent on the percentage removal of fluorine

was evaluated for both prepared adsorbents when the initial fluorine concentration was 10 mg/L, solution pH was 7, temperature was 303 K, contact time was 30 min and adsorbent dosage was 1.5 g. The obtained results are shown in Fig. 2, which indicate that for both adsorbents, the % removal of fluorine decreases from 93% to 65% and 77% to 96% for absorbents OPA and IGPA, respectively. This is occured when average particle size of adsorbent is increased. Since the smaller particles have higher surface area per unit mass and shortened diffusion paths, the penetration ability through the internal pores of adsorbent is very high. Therefore, for all the experiments, the average particle size was considered as 41.5 µm as the optimum particle size. The adsorbents such as green coloured marine algae (*Ulva fasciata*) [11], kikar (*Accia catechu* Willd), neem (*Azadirachta indica*), pipal (*Ficus religiosa*) [12] follows the same trend of decreasing particle sizes while increasing adsorption of fluoride.

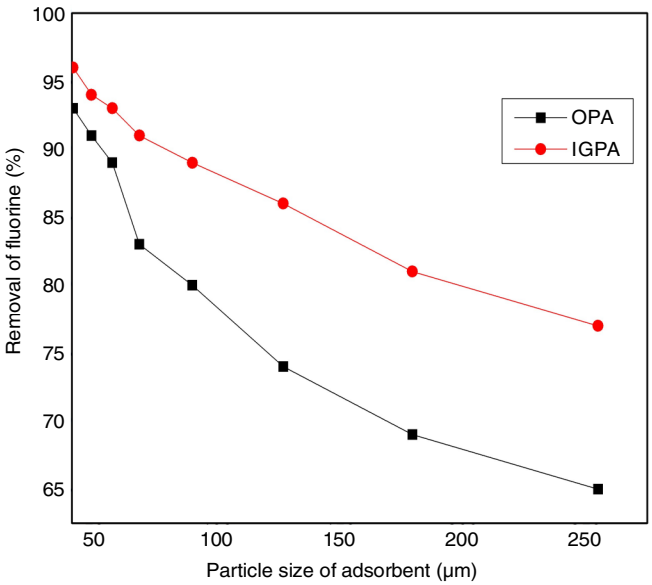

Fig. 2. Effect of particle size of both adsorbents on % removal of fluorine ions

Effect of contact time: The time allowed for the contact of fluoride molecules with adsorbent in the aqueous solution *i.e.* the contact time plays a significant role in the removal of fluoride. Fig. 3 shows the effect of contact time on percentage removal of fluoride for both adsorbents, it can be interpreted that, initially the % removal of fluorine was very rapid (from 0 to 88% and 0 to 91% for OPA and IGPA, respectively) with increase in the contact time from 0 to 15 min and the rate of removal decreases from 88 % to 94% in the case of OPA and 91% to 97% in the case of IGPA when contact time is increased from 15 to 60 min and finally, it becomes constant beyond a contact time of 60 min. The reason is attributed due to the enormous number of unoccupied sites available for adsorption in the early phases. As time progresses, the repulsive forces between the solute molecules become more prominent. There would be additional resistance for the adsorption process. Further, it was observed that with IGPA as adsorbent the adsorption was rapid at the initial stages compared with OPA.

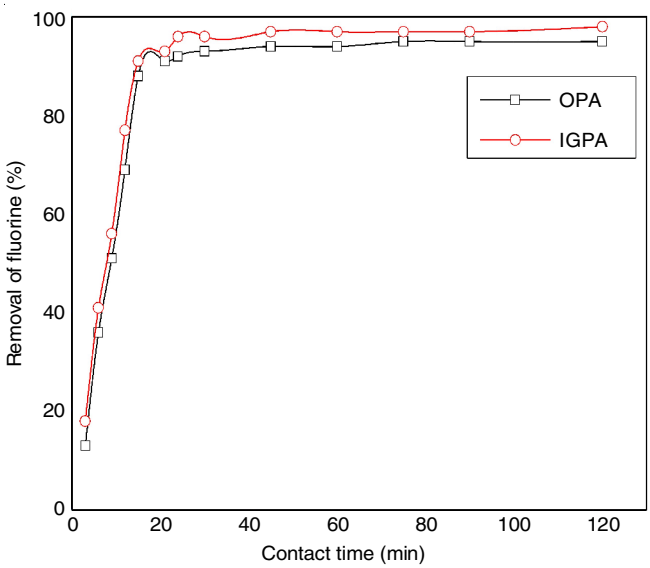

Fig. 3. Effect of contact time of process on % removal of fluoride ions

Effect of temperature: The effect of temperature on the fluoride removal was studied at varying temperatures from 35 to 60 ºC, while keeping the other parameters optimized. When temperature increased from 303 to 333 K, the percentage removal got increased from 93% to 98% in case of OPA and 96% to 99% in case of IGPA. Since, there is only a marginal increase in the % removal of flouride ions (5% and 3% for OPA and IGPA, respectively) (Fig. 4). So, the temperature does not play the significant role in the efficient removal of fluoride ions as the pyrolyzed leaves as adsorbent already get saturated, thus, the change in temperature caused least effect in this case. An increase in temperature leads to an increase in diffusivity of fluoride molecules and thus an increase in the adsorption rate can be observed [13]. This mechanism might confirmed that diffusion may be the rate-controlling in this process. In this case, the fluoride removal effectiveness of IGPA was superior to that of OPA.

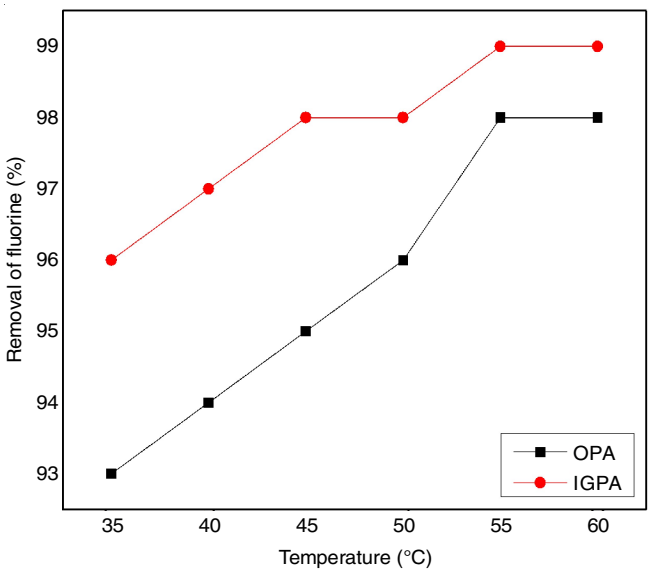

Fig. 4. Effect of temperature on % removal of fluoride ions

Effect of pH: The effect of pH on the % removal of fluoride ions for the adsorbents OPA and IGPA were analyzed at the varying pH of 2 to 12. From Fig. 5, in both cases, highest percentage of fluoride ion removal at pH was around 7 *i.e.* 92% for OPA and 96% for IGPA. When the pH decreased/increased, the % removal value became less. When the pH was increased or decreased, some unwanted ions such as H^+, Cl^-, SO_4^{2-}, CO_3^{2-}, Na^+, OH^-, *etc.* might interacted with the adsorption of fluoride onto the surface of OPA or IGPA. These unwanted ions might get adsorbed on the spores of the adsorbent in the place of fluoride molecules causing reduction in percentage removal.

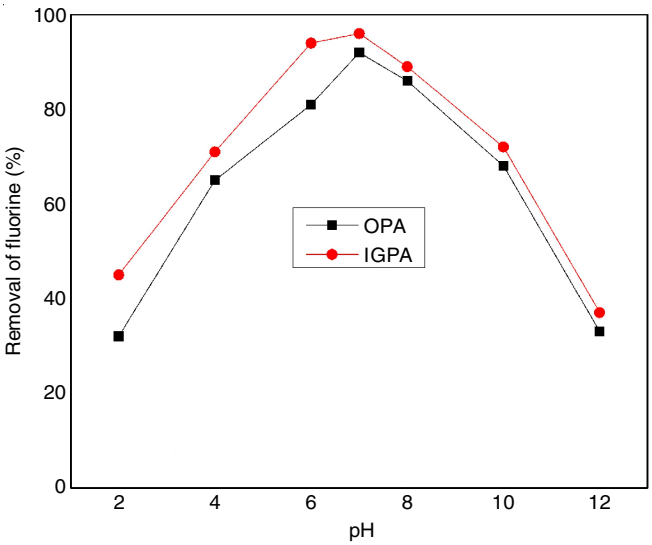

Fig. 5. pH of solution on % removal of fluoride ions

Adsorption isotherms: Batch studies were performed using both adsorbents separately at a constant temperature of 303 K and at pH 7 for 1.5 g dosage of average particle size adsorbent of 41.5 µm and at the initial concentration of fluoride at 10 ppm. Three isotherms models *viz*. Freundlich, Langmuir and Dubinin-Radushkevitch isotherms were used to examine an adsorbent's maximal sorption capacity. The plots of three studied isotherm models are shown in Fig. 6 and are respesented by the following equations:

$$Q_e = \frac{bQ_{max}C_e}{(1+bC_e)} \quad (1)$$

$$Q_e = KC_e^{1/n} \quad (2)$$

$$\ln Q_e = \ln Q_{max} - K_{ad}\varepsilon^2 \quad (3)$$

where Q_e amount of adsorbate in adsorbent at equilibrium, C_e equilibrium concentration and Q_{max}, b is the Langumir constants. Shape of the isotherms is described by the dimensionless equilibrium parameter, as $K_L = 1/(1 + b\ C_o)$. $K_L > 1$ is unfavourable, $0 < K_L < 1$is favourable, $K_L = 1$ is linear and $K_L = 0$ is irreversible. The K and n are the Freundlich constants, Q_{max} and K_{ad} are the D-R isotherm constants, which indicate the adsorption capacity and activity coefficient. Mean sorption energy is $E = (1/2K_{ad})^{1/2}$. The values of all the three isotherms parameters are given in Table-1.

TABLE-1
THE VALUES OF CONSTANT PARAMETERS OF THE STUDIED ADSORPTION ISOTHERM MODELS FOR FLUORIDE REMOVAL

Isotherm	Constant	Adsorbents	
		OPA	IGPA
Langmuir isotherm	b (L/mg)	2.91891	1.58703
	Q_{max} (mg/g)	0.51505	0.48477
	R^2	0.91893	0.95876
Freundlich isotherm	K ((mg/g)/(L/mg)$^{1/n}$)	0.30721	0.24648
	n (mg/g)	3.34194	2.93878
	R^2	0.82298	0.86416
Dubinin-Radushkevitch isotherm	q_s (mg/g)	0.48431	0.36955
	K_{ad}	-5.2×10^{-8}	-5.7×10^{-8}
	E (kJ/mol)	3.08	2.95
	R^2	0.932	0.903

From Table-1, it is clear that the adsorption of fluoride ions onto adsorbents OPA and IGPA follow Langmuir & Dubnin-Raduskevitch isotherm models. However, both prepared adsorbents are not fitted well with Freundlich, even R^2 value was not nearer to unity 'n' value which is greater than one. However, it is best fitted with D-R isotherm model as R^2 value was close to unity compared to the R^2 value of Langmuir isotherm model in case of OPA. For IGPA absorbent, Langmuir isotherm model is best fit when compared with D-R model. The shape of isotherm in case of Langumir isotherms is 0.033 and 0.059 of OPA and IGPA, respectively. The mean sorption energy are estimated as 3.08 and 2.95 for OPA and IGPA, respectively.

Thermodynamic studies: The assessed thermodynamic parameters are used in the determination of spontaneity, affinity

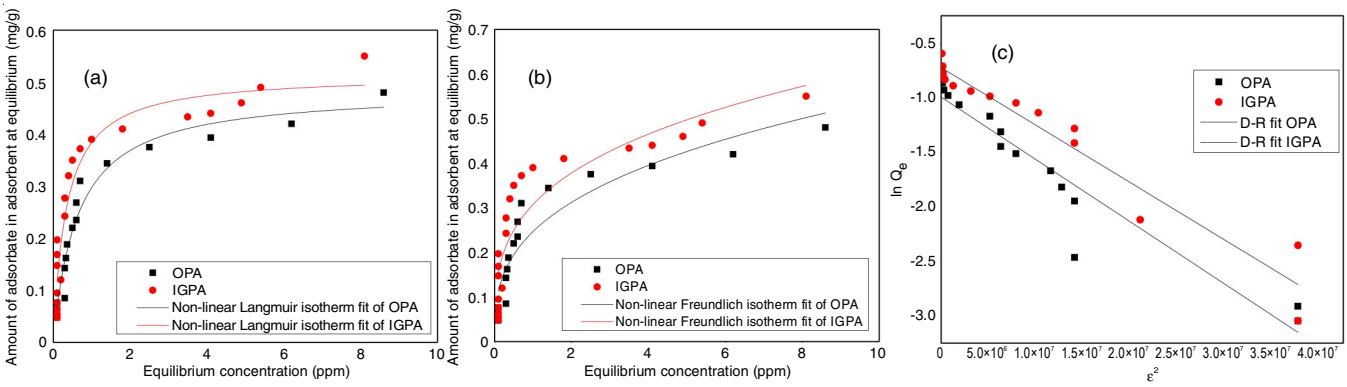

Fig. 6. Plots of Langmuir isotherm (a), Freundlich isotherm (b) and D-R isotherm (c) for fluoride ions adsorption onto OPA and IGPA

and heat change of the process. The relationship between three standard free energy change (ΔG_o) and equilibrium constant (K_a) is given by the following equation:

$$\Delta G_o = -RT \ln K_a \quad (4)$$

$$K_a = \frac{q_{eq}}{C_{eq}} \quad (5)$$

where q_{eq} is the amount of removed fluoride ions and C_{eq} is the equilibrium adsorbate concentration in the solution.

The enthalpy change (ΔH_o) and the entropy change (ΔS_o) were estimated in distinction to the following equation:

$$\ln K_a = \frac{\Delta S_o}{R} - \frac{\Delta H_o}{RT} \quad (6)$$

$$\Delta G_o = \Delta H_o - T\Delta S_o \quad (7)$$

The slope and intercept of the linear vant Hoff plot ln (q_{eq}/C_{eq}) *vs*. (1/T) were used to calculate the values of ΔH and ΔS [14,15].

The ΔH_o and ΔS_o values for both adsorbents *i.e*. OPA and IGPA were found to be positive (Table-2). This shows that the adsorption process was endothermic, with the adsorbent having a stronger affinity for fluoride ions and increasing unpredictability at the solid-solute interface. The chemical and physical sorption can be distinguished using the enthalpy values of the sorption process [16]. Enthalpy values for chemical sorption range from 83 to 830 kJ mol^{-1}, whereas those for physical sorption range from 8 to 25 kJ mol^{-1}. Based on the contrast made above, the fluoride ions sorption by both OPA and IGPA appears to be essentially a chemical process.

The values of ΔG° (Gibb's free energy) were positive (except at 328 and 333 K) for lower temperatures (303 to 323 K). The adsorbent of OPA, which indicates the reaction is non-spontaneous. In case of IGPA, ΔG° values were negative (except 303 K) showing the reaction to be spontaneous. A decreasing trend in ΔG° value when temperature was increased indicates the increasing temperature that favours the adsorption process for this adsorbent.

Kinetics studies: The pseudo-second order parameters were estimated by plotting t/Q_e and contact time (t). From Fig. 7, it is deciphered that both adsorbents are fit perfectly with the pseudo-second order fit with coefficient of regression 0.989 and 0.978 for IGPA and OPA, respectively. The stimated values and experiment values of Q_e for IGPA and OPA were 0.348, 0.347 and 0.327, 0.317 respectively.

Surface characterization of adsorbents

FE-SEM studies: The FE-SEM micrographs were used to examine the morphological characteristics of *Annona squamosa* (custard apple leaves) leaves adsorbents before and after fluoride ion adsorption. Fig. 8(a-b) shows the FE-SEM micrograph of OPA and IGPA adsorbents, before adsorption. These images show that the adsorbent is highly heterogeneous and that the surface shape of the adsorbent is rough, suggesting that the fluoride ion might be adsorbed. Whereas Fig. 8(c-d) shows the FE-SEM micrographs OPA and IGPA respectively, after the adsorption of fluoride ion onto the adsorbent.

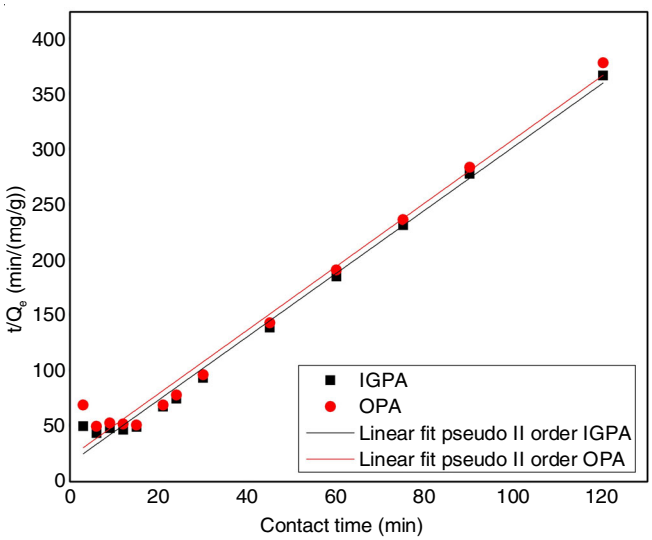

Fig. 7. Linear fit of pseudo second order of adsorbents OPA and IGPA

When compared to FE-SEM images before adsorption [Fig. 8(a-b)], it is evident that the surface texture of OPA and IGPA is completely changed after adsorption of fluoride ions. The surface of a fluoride ions loaded adsorbent clearly indicates that fluoride ions cover the surface of adsorbent [Fig. 8(c-d)]. After the fluoride ion adsorption, the pores were entirely filled with fluoride molecules and appeared smooth. This finding implies that fluoride ions is adsorbing to the functional groups found within the pores. During the fluoride ions adsorption, the adsorbents' surfaces became smooth. The adsorption of fluoride ions on the pores of the adsorbent causes the surface to smooth out. It's also possible that this is related to the adsorbent's decreased the surface heterogeneity.

FTIR studies: Since, the fluoride adsorption took place onto the adsorbent's surface, some of the absorption peaks were shifted and new peaks appeared. In case of OPA, it is evident that the characteristic peak of –OH stretching vibration was shifted from 3380.79 cm^{-1} to 3379.37 cm^{-1}, which shows the increase in free hydroxyl functional group as a result of the interaction between fluoride ions and OH groups of adsorbent (Fig. 9a-b). The peak of CH stretching of alkenes at 2922 cm^{-1} was shifted to 2921 cm^{-1}. The peak at 1633 cm^{-1} was shifted to 1616 cm^{-1} due to the presence of carbonyl groups. The absorption peaks at 1435, 1259, 1069, 1037 cm^{-1} were shifted to

TABLE-2
THERMODYNAMIC PARAMETERS VALUES FOR FLUORIDE IONS ADSORPTION ONTO OPA AND IGPA

Adsorbent	ΔH_o (KJ/mol)	ΔS_o (J/mol K)	ΔG_o (kJ/mol)					
			308 K	313 K	318 K	323 K	328 K	333 K
OPA	49.46211	0.152826	2.09	1.69	1.21	0.6	-1.34	-1.36
IGPA	50.9042	0.163403	0.57	-0.19	-1.30	-1.31	-3.26	-3.30

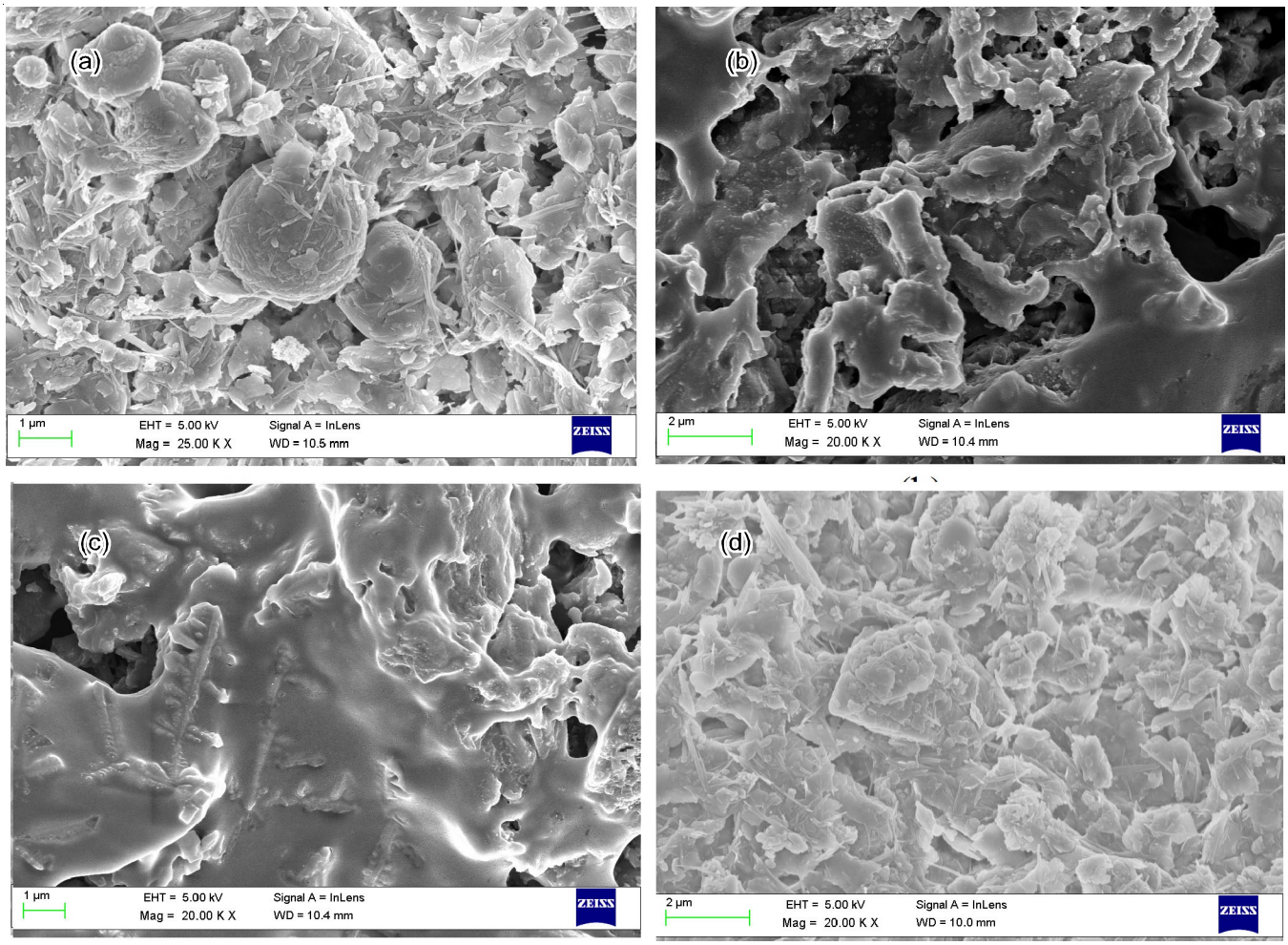

Fig 8. FE-SEM micrographs of OPA and IGPA before (a,b) and after (c,d) adsorption of fluoride ions onto its surface

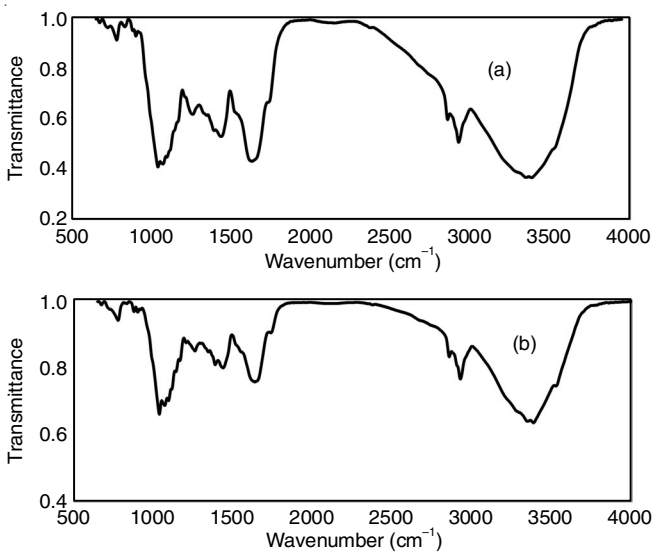

Fig. 9. FTIR spectra of adsorption of fluoride ions adsorption onto OPA before (a) and after (b) adsorption

1432, 1255, 1068 and 1036 cm^{-1}. These changes indicate the adsorption of fluoride ions onto the surface of OPA. The existing peaks was disappeared at 1385, 1093 cm^{-1} indicates the involvement of the chemical reactions during adsorption.

The FTIR spectra of IGPA before and after adsorption of fluoride ions are shown in Fig. 10a-b. Some of the absorption peaks were shifted and disappeared and new peaks were formed due to the fluoride adsorption onto adsorbent surface. It is evident from this figure that the characteristic peak at OH stretching vibration appeared at 3619 cm^{-1} in before and after adsorption spectra, whereas the peaks at 3529 and 3380 cm^{-1} that got disappeared, which corresponds to –OH stretching. This shows that the increase of free hydroxyl groups due to the interaction of fluoride ions and OH groups present in the adsorbent. The peak of NH stretching at 2928 cm^{-1} got shifted to 2925 cm^{-1} while the peak of NH at 2900 cm^{-1} disappeared. The calcium carbonate and the anhydride peaks were appeared at 2513 cm^{-1} and 1796 cm^{-1}, respectively. These changes indicate that the adsorption of fluoride ions onto the surface of IGPA and also the involvement of chemical reactions during the adsorption.

XRD analysis: The XRD patterns of the both adsorbents OPA and IGPA before and after treatment with fluoride ions are shown in Figs. 11a-b and 12a-b, respectively. It is observed that some significant changes in the crystal structure of XRD pattern after the adsorption of fluoride solution occured. The XRD pattern in Fig. 11a-b showed the prominent peaks with 2θ values of 20.7º, 26.7º, 29.4º and 39.4º for OPA, whereas

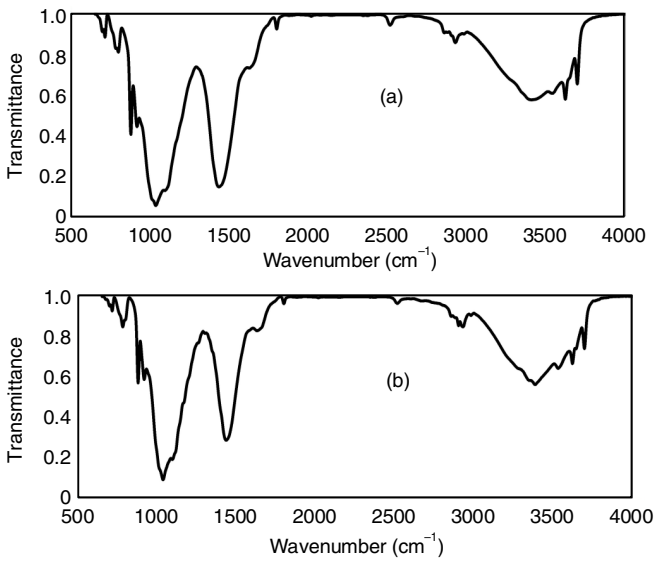

Fig. 10. FTIR adsorption spectra of fluoride ions adsorption onto IGPA before (a) and after (b) adsorption

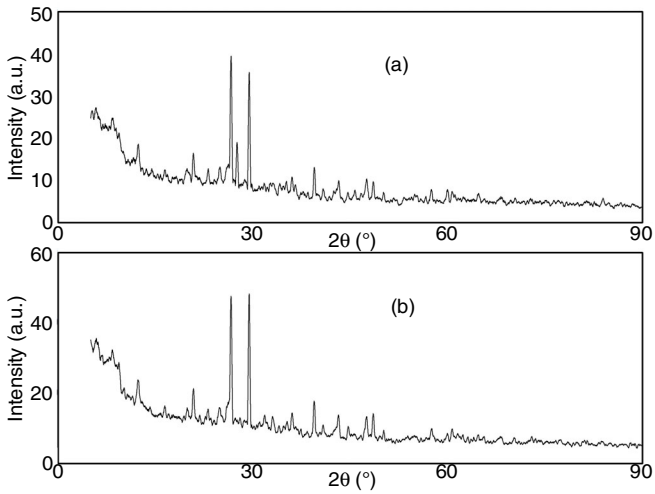

Fig. 11. XRD patterns before (a) and after (b) adsorption of adsorbent OPA

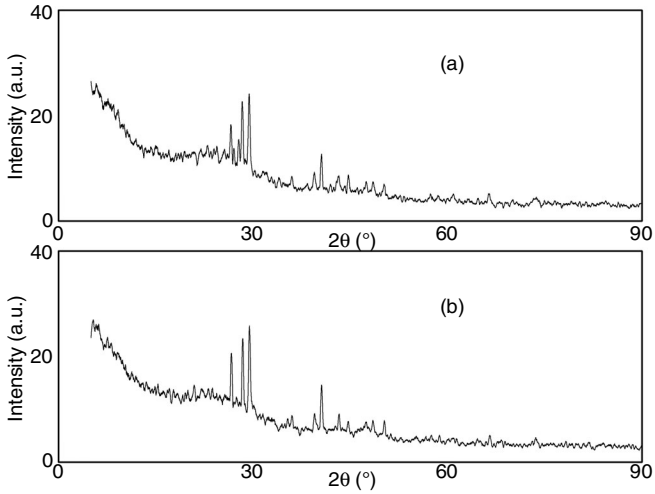

Fig. 12. XRD patterns before (a) and after (b) adsorption of adsorbent IGPA

the IGPA prominent peaks with 2θ values of 26.7º, 28.4º, 29.4º and 40.5º have been shown in Fig. 12a-b. Both adsorbents are close with reduction in the intensity of the peaks describe the fluoride ion deposited on the OPA and IGPA surface. Only one peak with 2θ value of 27.5º and 27.8º is removed after the adsorption incase of OPA and IGPA, respectively.

Conclusion

The pyrolyzed materials (biochar) obtained from the leaves of custard apple (*Annona squamosa*) at 800 ºC (OPA) in open air and in presence of inert gas (IGPA) were used as adsorbent materials for the successful removal of fluoride ions using batch studies. The studies showed that both adsorbents (OPA and IGPA) have comparable fluoride ions adsorption capacity at the optimized conditions. The results of this investigation were well described by pseudo-second-order kinetic models and fitted by the isotherms such as Langmuir and D-R models and the process was found to be spontaneous and endothermic. Adsorption process of OPA and IGPA in aqueous solution occurs through the chemisorptions and well-explained by the higher enthalpy changes and the XRD results.

CONFLICT OF INTEREST

The authors declare that there is no conflict of interests regarding the publication of this article.

REFERENCES

1. S. Nizam, H.S.Virk and I.S. Sena, *Environ. Adv.*, **8**, 100200 (2022); https://doi.org/10.1016/j.envadv.2022.100200
2. L.H. Kelly, F.A. Uzal, R.H. Poppenga, H. Kinde, A.E. Hill, W.D. Wilson, and B.T. Webb, *J. Vet. Diagn. Invest.*, **32**, 942 (2020); https://doi.org/10.1177/1040638720962746
3. S.R. Lakshmi Prasad, V.V. Reddy and N.K. Swamy, *Nat. Environ. Pollut. Technol.*, **8**, 789 (2009).
4. A.K. Haritash, A. Aggarwal, J. Soni, K. Sharma, M. Sapra and B. Singh, *Appl. Water Sci.*, **8**, 52 (2018); https://doi.org/10.1007/s13201-018-0691-0
5. P. Mondal and S. George, *Rev. Environ. Sci. Biotechnol.*, **14**, 195 (2015); https://doi.org/10.1007/s11157-014-9356-0
6. M. Habuda-Stanic, M.E. Ravancic and A. Flanagan, *Materials*, **7**, 6317 (2014); https://doi.org/10.3390/ma7096317
7. J. Saleem, U.B. Shahid, M. Hijab, H. Mackey and G. McKay, *Biomass Conv. Bioref.*, **9**, 775 (2019); https://doi.org/10.1007/s13399-019-00473-7
8. A.K. Tolkou, N. Manousi, G.A. Zachariadis, I.A. Katsoyiannis and E.A. Deliyanni, *Sustainability*, **13**, 7061 (2021); https://doi.org/10.3390/su13137061
9. M.S. Reza, C.S. Yun, S. Afroze, N. Radenahmad, M.S.A. Bakar, R. Saidur, J. Taweekun and A.K. Azad, *Arab J. Basic Appl. Sci.*, **27**, 208 (2020); https://doi.org/10.1080/25765299.2020.1766799
10. G. Yin, Z. Liu, Q. Liu and W. Wu, *Chem. Eng. J.*, **230**, 133 (2013); https://doi.org/10.1016/j.cej.2013.06.085
11. G. Babu Rao, G. Kalyani, B. Vijaya Saradhi and Y. Prasanna Kumar, *Nature Environ. Pollut. Technol.*, **8**, 231 (2009).
12. S. Goyal and A. Sharma, *Int. J. Eng. Res. Technol.*, **3**, 870 (2014).
13. F.A. Pavan, A.C. Mazzocato and Y. Gushikem, *Bioresour. Technol.*, **99**, 3162 (2008); https://doi.org/10.1016/j.biortech.2007.05.067
14. S. Meenakshi, C.S. Sundaram and R. Sukumar, *J. Hazard. Mater.*, **153**, 164 (2008); https://doi.org/10.1016/j.jhazmat.2007.08.031
15. B.V. Gopal and K.P. Elango, *J. Hazard. Mater.*, **141**, 98 (2007); https://doi.org/10.1016/j.jhazmat.2006.06.099
16. Y. Ho and G. McKay, *Process Saf. Environ. Prot.*, **76**, 332 (1998); https://doi.org/10.1205/095758298529696